AN ELECTROCHEMICAL STUDY OF THE COBALT ELECTRODEPOSITION ONTO A CARBON FIBER ULTRAMICROELECTRODE

JAIR A. CORONA-CASTRO [1], GIAAN A. ÁLVAREZ-ROMERO [1], MARGARITA RIVERA [2], CLARA H. RIOS-REYES [3], L.E. BAÑUELOS-GARCÍA [4], E. GARCÍA-SÁNCHEZ [4] AND LUIS H. MENDOZA-HUIZAR [1]*

[1]*Universidad Autónoma del Estado de Hidalgo, Academic Area of Chemistry, Carretera Pachuca-Tulancingo Km. 4.5 Mineral de la Reforma, México.*
[2]*Instituto de Física, Universidad Nacional Autónoma de México, Ciudad de México, 04510, México.*
[3]*Universidad La Salle Pachuca, Calle Belisario Domínguez 202, Centro, Pachuca de Soto, Hgo., 42000, México.*
[4]*Universidad Autónoma de Zacatecas, Unidad Académica de Ingeniería Eléctrica, Av. Ramón López Velarde 801, Zacatecas, 98600, México.*

ABSTRACT

A kinetic study of the cobalt electrodeposition onto a carbon fiber ultramicroelectrode of 11 µm of diameter was conducted in overpotential conditions from an aqueous solution containing 0.01 M $CoCl_2$ + 0.1 M NH_4Cl. From the voltamperometric and chronoamperometric studies, it was found that the value of the diffusion coefficient is $1.2x10^{-5}$ cm^2 s^{-1}. The analysis of the current density transients suggests that cobalt electrodeposition onto a carbon fiber electrode follows an instantaneous nucleation process controlled by spherical diffusion mass transport. Also, the number of active nucleation sites increases as the applied potential decreases.

Keywords: Cobalt, electrodeposition, ultramicroelectrode, carbon fiber.

INTRODUCTION

Cobalt electrodeposits have received considerable attention due to their potential applications in scientific and technological fields related to the storage of digital information.[1] They have been used in the fabrication of sensors,[2] heterogeneous catalysis,[3] and in the synthesis of intercalation compounds for energy storage[4] among others. Here, it is interesting to mention that during the cobalt electrodeposition process it is possible to optimize parameters such as temperature, applied current density, and electrolyte composition.[5] In this sense, Co electrodeposition has been studied onto different substrates such as: GCE,[6–10] Cu,[11–14] Au,[15–17], stainless steel,[6,18] Al[19–21] and Pt[22,23] and from plating baths based on sulfates, [9,11,13–15,24] chlorides, [16–18, 25,] and citrates[8] solutions, mainly. The results obtained from different systems indicate that cobalt electrodeposition follows a progressive nucleation, but it may switch to instantaneous if ultrasound is employed to improve the mass transfer,[26] or increasing the cobalt concentration in the plating bath.[27] Also, cobalt electrodeposition may also occur via a nucleation process under charge transfer control.[28] Thus, cobalt electrodeposition is diffusional controlled, but a mixed control has been found as well[22]. In addition, different shape morphologies, such as fractals, butterfly, dendrites, snowflake-like, which exhibit different properties may be obtained[5]. Here it is interesting to mention that materials based on cobalt has been scarcely synthesized onto nano or ultramicroelectrodes (UME's) by electrodeposition,[29–34] despite their advantages. For example, the UME's reduced dimensions allow the formation and growth of a limited number of nuclei or even single nucleus, minimizing the interference between neighboring nuclei. Also, the effects of small variations in the surface area of the substrate can be detected in electrochemical measurements.[35] Moreover, UMEs allow a faster double-layer charging, reduced ohmic loss, and high mass-transport rates[36]. Moreover, the use of UME's offers advantages such as the formation of a single core with controlled morphology and size, which leads to precise control of the electronic, chemical, and optical properties of the synthesized material. Thus, in this work we studied the cobalt electrodeposition process onto a carbon fiber of 11 µm (C-UME) employing cyclic voltammetry and potentiostatic techniques.

METHODOLOGY

Co electrodeposits onto an UME of carbon fiber (C-UME) from the plating bath containing 0.01 M $CoCl_2$ + 0.1 M NH_4Cl were carried out. All solutions were prepared using analytical grade reagents with ultrapure water (Millipore-Q system). The working electrode was a carbon fiber ultramicroelectrode of 11 µm diameter, the exposed surface was polished with water over a Fandelli 2000 sandpaper. A platinum wire was used as a counter electrode. All potentials are reported against an Ag/AgCl electrode. All electrochemical experiments were performed on an EPSILON potentiostat-galvanostat connected to a personal computer running Epsilon EC software to allow the experiment control and data acquisition.

RESULTS AND DISCUSSION

Voltamperometric study

Figure 1 shows a typical cyclic voltammogram recorded from the system C-UME/ 0.01 M $CoCl_2$ + 0.1 M NH_4Cl, at the scan rate of 30 mV s^{-1}. The scanning started in the null current zone where not electrochemical processes were recorded. Note at direct scan, the formation of a peak *A* at -0.760 V while that during the inverse of the potential scan, it is possible to observe the formation of a crossover, EC_1, which is typical of the formation of a new phase involving a nucleation process.[19] In the anodic zone, it is possible to observe the formation of a main peak B which has been associated with the dissolution of cobalt phase previously electrodeposited during the direct scan.[20] Furthermore, a cyclic voltammetric measurement in the C-UME immersed in an aqueous solution containing just the supporting electrolyte, 0.1 M NH_4Cl, did not show the presence of the peak A (broken line in Figure 1), which indicates that this electrochemical signal is due the cobalt reduction process.

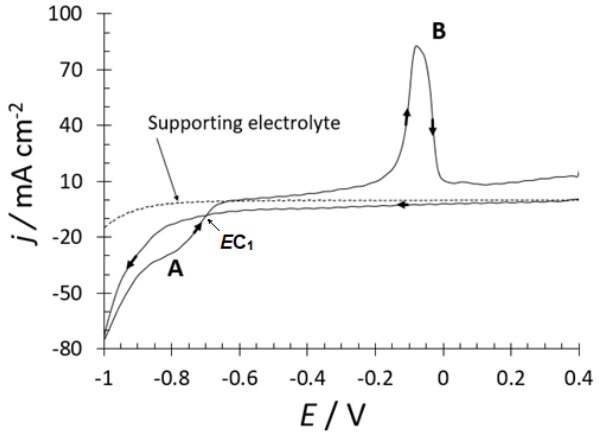

Figure 1. A comparison of two cyclic voltammetric curves obtained from the C-UME/ x M $CoCl_2$ + 0.1 M NH_4Cl system at two different $CoCl_2$ concentrations (a) x=0 (- -) and (b) $x=10^{-2}$ M (—). The potential scan was started at 0.400 V toward the negative direction with a scan potential rate of 30 mV s^{-1}. Arrows indicate the potential scan direction. Cathodic current density peaks (A) and anodic peak (B) are also indicated in the figure.

Fig. 2 shows a set of cyclic voltammograms obtained from the system C-UME / 0.01 M $CoCl_2$ + 0.1 M NH_4Cl at different potential scan rates. Here, it is interesting to note that the potentials where appears the peaks A and B remains approximately constant.

**Corresponding author email: hhuizar@uaeh.edu.mx*

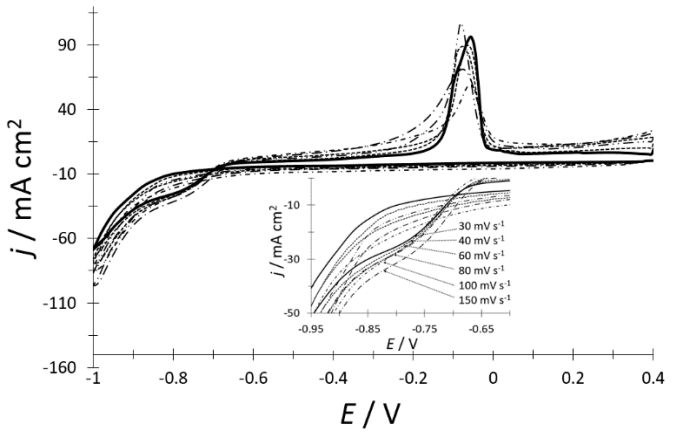

Figure 2. Typical cyclic voltammograms obtained from the C-UME/ 0.01 M $CoCl_2$ + 0.1 M NH_4Cl system at different scan potential rates indicated in the Figure. In all cases, the potential scan was started at 0.4 V toward the negative direction to -1. V.

In order to determine the type of kinetic control during the cobalt electrodeposition process, the cathodic peak current was plotted against the scan rate at ½, see Figure 3. A linear relationship was found indicating a diffusional-controlled process[37]. From the slope of the j_p vs $v^{1/2}$ plot and the Berzins–Delahay's equation[37] it was possible to evaluate the diffusion coefficient value as $1.2x10^{-5} \pm 5.3x10^{-8}$ cm^2 s^{-1}.

$$j_p = 0.6105\left(\frac{F^3}{RT}\right)^{1/2} n^{3/2} D^{1/2} C_0 v^{1/2} \quad (1)$$

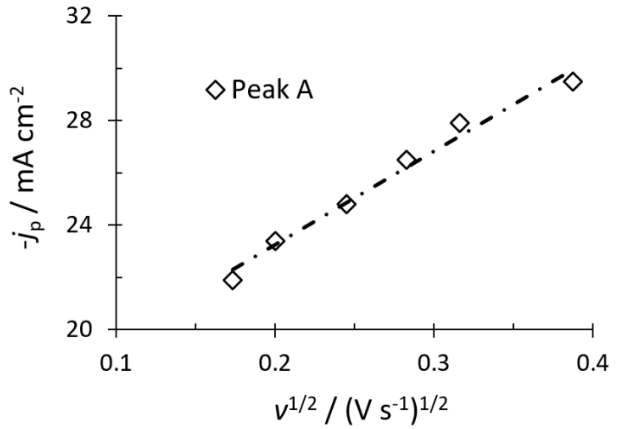

Figure 3. Plot of the experimental cathodic peak current density (j_p) as a function of scan rate ($v^{1/2}$) for peak A (see Figure 2). The straight line corresponds to the linear fit to the experimental data.

Also, the kinetic parameters associated with the $Co^{2+} + 2e \leftrightarrow Co^0$ process in the present system were evaluated by means the Tafel equations, equation (2) and (3).[36]

$$\ln j_c = \ln j_0 - \frac{\alpha_c nF}{RT} \quad (2)$$

$$\ln j_a = \ln j_0 + \frac{(1-\alpha_c) nF}{RT} \quad (3)$$

In these equations j_c and j_a are the cathodic and anodic current respectively, j_0 is the exchange current, α_C is the cathodic transfer coefficient, while the anodic transfer coefficient is α_a =1- α_C. In Figure 4 are depicted the plots of the logarithm of the cathodic and anodic current vs. the applied potential according to equations (2) and (3). The anodic and cathodic branch data were obtained from a linear voltammogram recorded at a scan rate 1 mV s^{-1} from the C-UME/ 0.01 M $CoCl_2$ + 0.1 M NH_4Cl system. Fitting the linear part of these branches to the Tafel equations, yielded a value of the cathodic transfer coefficient of 0.23, while the anodic transfer coefficient is 0.77. The above suggests that the anodic process is favored in the present system.

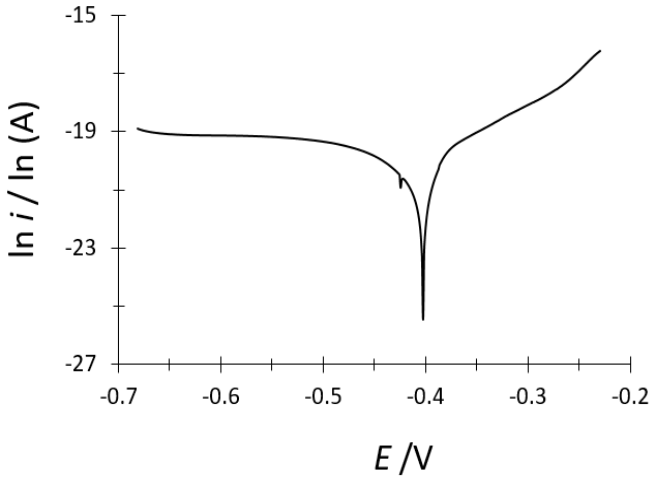

Figure 4. Tafel plots for the current recorded from the C-UME/ 0.01 M $CoCl_2$ + 0.1 M NH_4Cl system at a scan rate 1 mV s^{-1}.

Potentiostatic study

Formation of new phases generally occurs through nucleation and growth mechanisms and the corresponding current transients can provide valuable information about the kinetics of electrodeposition. Figure 5 shows a set of current density transients recorded at different potentials by pulse potential technique (solid lines). These transients were obtained by applying an initial potential (E_0) of 0.400 V on the electrode surface. At this potential value, the cobalt deposition had still not begun, see Figure 1. After the application of this initial potential, a step of negative potential (E_c) was varied on the electrode surface in the potential range [-0.8 to -1 V] for 32 s. From Figure 5, (solid lines), it may be observed that at shorter times there is a falling current transient. Note that after this falling current, in each case, the *j*/*t* plot increases and passes through a maximum. Similar current density transients have been related to an instantaneous nucleation controlled by spherical diffusion mass transport to a micro-disc[38,39]. The theoretical model that describe these kind of current density transients is given by the following equation:[38,39].

$$j(t) = (4nFDc^{\infty}r + 8nFc^{\infty}r^2 D^{1/2}\pi^{-3/2}t^{-1/2})[1 - \exp(-N\pi kDt)] \quad (5)$$

Thus, the experimental transients (solid lines) represented in Figure 5 were fitted from a nonlinear fit to equation (5). From Figure 5 it can be seen that the theoretical transients (dashed lines) generated through equation (5) compare favorably with the experimental ones obtained at different potential steps, suggesting that this model is able to predict the overall behavior of the experimental transient.

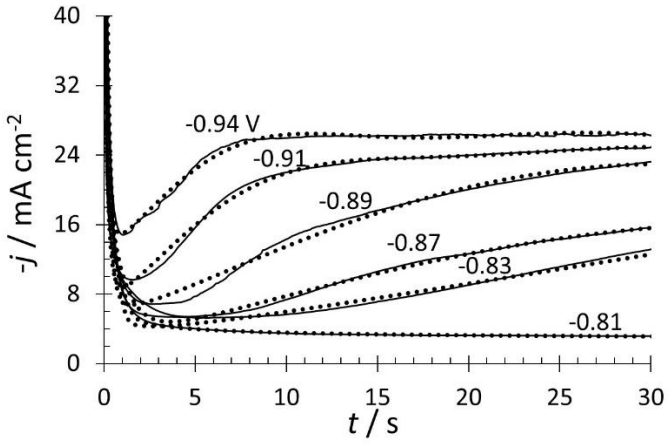

Figure 5. a) A set of experimental current transients recorded from the C-UME/ 0.01 M $CoCl_2$ + 0.1 M NH_4Cl system by means of the double potential step technique (solid lines) and the theoretical transients (●●●) obtained by a non-linear fit of Eq. (5) to the experimental data.

From these fittings, the values of the kinetic parameters associated with the nucleation and growth process of Co on the C-UME were determined and they are reported in Table 1. Note that, as the potential values decrease, the number of active sites, N_0, increases. However, the value of the diffusion constant remains constant, with an average value of $1.2x10^{-5}$ cm^2 s^{-1}. This coefficient diffusion value compares favorably with the obtained from the voltamperometric study.

Table 1. Kinetic parameters of Co electrodeposition from the C-UME/ 0.01 M $CoCl_2$ + 0.1 M NH_4Cl system.

E / V	N_0x10^{-5} / cm^{-2}	$Dx10^5$ / cm^2 s^{-1}
-0.81	0.270	1.315
-0.83	0.916	1.198
-0.87	2.081	1.130
-0.89	1.874	1.335
-0.91	3.558	1.140
-0.94	4.587	1.038

CONCLUSIONS

An electrochemical study on the cobalt electrodeposition process onto a carbon fiber microelectrode from an aqueous solution containing 0.01 M $CoCl_2$ + 0.1 M NH_4Cl in overpotential conditions has been carried out through voltammetric and potentiostatic studies. The analysis of the voltammetric curves at different scan rates potential indicated that the cobalt electrodeposition process is diffusion controlled and the value of the diffusion coefficient is $1.2x10^{-5}$ cm^2 s^{-1}. It was also possible to evaluate the anodic (α_a) and cathodic (α_c) transfer coefficients; a higher value of α_a =0.77 compared to α_c =0.23 means that the anodic process is favored in the present system. The potentiostatic study indicated that the electrodeposition of cobalt onto a carbon fiber electrode follows an instantaneous nucleation process, which is controlled by spherical diffusion mass transport to the ultramicroelectrode. Also, the number of active nucleation sites increases with the decrease of the applied potential.

ACKNOWLEDGMENTS.

Authors gratefully acknowledge financial support from CONACYT (project CB2015-257823) and to the Universidad Autónoma del Estado de Hidalgo. JACC acknowledges CONACYT for the scholarship granted for Doctoral studies and LHMH acknowledges to the SNI for the distinction of his membership and the stipend received.

REFERENCES

1. H. Y. Ho, W. Bin Chen, T. Y. Fu, S. J. Chen, *IEEE Trans. Magn.* **50**, 1, (2014)
2. H. Yamaura, J. Tamaki, K. Moriya, N. Miura, N. Yamazoe, *J. Electrochem. Soc.* **144,** L158, (1997).
3. P. Nkeng, J. F. Koenig, J. L. Gautier, P. Chartier, G. Poillerat, *J. Electroanal. Chem.* **402,** 81 ,(1996).
4. K. Ramachandran, C. O. Oriakhi, M. M. Lerner, V. R. Koch, *Mater. Res. Bull.* **31**, 767, (1996).
5. X. Liu, R. Yi, Y. Wang, G. Qiu, N. Zhang, X. Li, *J. Phys. Chem. C* **111,** 163, (2006).
6. N. Ramos Lora, L. H. Mendoza Huizar, C. Hilda Rios-Reyes, C. A. Galán-Vidal, Adv. Mat. Res. **976**, 144, (2014).
7. M. Palomar-Pardavé, J. Aldana-González, L. E. Botello, E. M. Arce-Estrada, M. T. Ramírez-Silva, J. Mostany, M. Romero-Romo, *Electrochim. Acta* **241,** 162, (2017).
8. A. C. Frank, P. T. A. Sumodjo, *Electrochim. Acta* **132**, 75, (2014).
9. Y. Song, Z. He, H. Zhu, H. Hou, L. Wang, *Electrochim. Acta* **58**, 757, (2011).
10. C. H. Rios-Reyes, L. H. Mendoza-Huizar, M. Rivera, *J. Solid State Electrochem.* **14**, 659, (2010).
11. F. Pagnanelli, P. Altimari, M. Bellagamba, G. Granata, E. Moscardini, P. G. Schiavi, L. Toro, *Electrochim. Acta* **155,** 228, (2015).
12. H. Harti, J. L. Bubendorff, A. Florentin, C. Pirri, J. Ebothe, *J. Cryst. Growth* **319,** 79, (2011).
13. S. Banbur-Pawlowska, K. Mech, R. Kowalik, P. Zabinski, *Appl. Surf. Sci.* **388**, 805, (2016).
14. M. A. M. Ibrahim, R. M. Al Radadi, *Mater. Chem. Phys.* **151**, 222, (2015).
15. V. P. Graciano, U. Bertocci, G. R. Stafford, *J. Electrochem. Soc.* **166,** D3246, (2019).
16. D. Lützenkirchen-Hecht, D. Hamulić, R. Wagner, I. Milošev, *Radiat. Phys. Chem.* **175**, 108113, (2020).
17. L. H. Mendoza-Huizar, J. Robles, M. Palomar-Pardavé, *J. Electroanal. Chem.* **545**, 39, (2003).
18. M. Ohba, T. Scarazzato, D. C. R. Espinosa, J. A. S. Tenório, Z. Panossian, *Miner. Met. Mater. Ser.* **148**, 967 (2019).
19. B. R. Tzaneva, A. I. Naydenov, S. Z. Todorova, V. H. Videkov, V. S. Milusheva, P. K. Stefanov, *Electrochim. Acta* **191**, 192, (2016).
20. P. G. Schiavi, P. Altimari, R. Zanoni, F. Pagnanelli, *Electrochim. Acta* **220**, 405, (2016).
21. P. G. Schiavi, P. Altimari, F. Pagnanelli, E. Moscardini, L. Toro, *Chem. Eng. Trans.* **43** 673, (2015).
22. E. Herrero, J. Li, H. D. Abruña, *Electrochim. Acta* **44,** 2385, (1999).
23. F. R. Bento, L. H. Mascaro, *J. Braz. Chem. Soc.* **13,** 502, (2002).
24. C. H. Rios-Reyes, L. H. Mendoza-Huizar, M. Rivera, *J. Solid State Electrochem. 2009 144*(**14),** 659, (2009).
25. M.I. Cruz-Martinez, M. Rivera, G.A. Álvarez-Romero, S. Nieto-Velázquez, L.H. Mendoza-Huizar. Pädi **9**, 145, (2021).
26. S. Floate, M. Hyde, R. G. Compton, *J. Electroanal. Chem.* **523**, 49, (2002).
27. N. Myung, K.H. Ryu, P.T.A. Sumodjo, K. Nobe, Electrochemical Society Proceedings, PV 97-27, 136, (1998).
28. S. S. Abd El Rehim, M. A. M. Ibrahim, M. M. Dankeria, *J. Appl. Electrochem.* **32**, 1019, (2002).
29. L. Philippe, N. Kacem, J. Michler, *J. Phys. Chem. C* **111**, 5229, (2007).
30. Z. Jin, A. J. Bard, *PNAS* **117**, 12651, (2020).
31. Q. Cheng, J. Tang, H. Zhang, L. C. Qin, *Chem. Phys. Lett.* **616**–**617**, 35, (2014).
32. J. Wen, B. Xu, J. Zhou, *Nano-Micro Lett.* **11**, 1, (2019).
33. V. Brasiliense, J. Clausmeyer, P. Berto, G. Tessier, C. Combellas, W. Schuhmann, F. Kanoufi, *Anal. Chem.* **90**, 7341, (2018).
34. V. Brasiliense, J. An Clausmeyer, A. L. Dauphin, J.-M. No• l, P. Berto, G. Tessier, O. Schuhmann, F. Kanoufi,] V Brasiliense, A. L. Dauphin, J.-M. No• l, F. Kanoufi, J. Clausmeyer, R. W. Schuhmann, P. Berto, et al., *Angew. Chemie Int. Ed.* **56** ,10598, (2017).
35. M. J. Peña, R. Celdran, R. Duo, *J. Electroanal. Chem.* **367**, 85, (1994).
36. A. J. Bard, L. R. Faulkner, *Electrochemical methods and applications*, 2nd ed., John Wiley & Sons, Ltd, 2001.
37. T. Berzins, P. Delahay, *J. Am. Chem. Soc.* **75**, 555, (1953).
38. A. N. Correia, S. A. S. Machado, J. C. V. Sampaio, L. A. Avaca, *J. Electroanal. Chem.* **407**, 37, (1996).
39. A. N. Correia, L. A. Avaca, S. A. S. Machado, L. H. Mazo, C. R. Alves, S. M. Silva, A. L. R. Nobre, R. M. Martins, *Quim. Nova* **21**, 78, (2005).